sustainability

Article

A Computationally Efficient Rule-Based Scheduling Algorithm for Battery Energy Storage Systems

Lorenzo Becchi [1], Elisa Belloni [2], Marco Bindi [1], Matteo Intravaia [1,*], Francesco Grasso [1], Gabriele Maria Lozito [1] and Maria Cristina Piccirilli [1]

1 Department of Information Engineering, Università degli Studi di Firenze, Via di Santa Marta 3, 50139 Firenze, Italy; lorenzo.becchi@unifi.it (L.B.); m.bindi@unifi.it (M.B.); francesco.grasso@unifi.it (F.G.); gabrielemaria.lozito@unifi.it (G.M.L.); mariacristina.piccirilli@unifi.it (M.C.P.)

2 Department of Engineering, Università di Perugia, Via G. Duranti n.93, 06125 Perugia, Italy; elisa.belloni@unipg.it

* Correspondence: matteo.intravaia@unifi.it

Abstract: This paper presents a rule-based control strategy for the Battery Management System (BMS) of a prosumer connected to a low-voltage distribution network. The main objective of this work is to propose a computationally efficient algorithm capable of managing energy flows between the distribution network and a prosumer equipped with a photovoltaic (PV) energy production system. The goal of the BMS is to maximize the prosumer's economic revenue by optimizing the use, storage, sale, and purchase of PV energy based on electricity market information and daily production/consumption curves. To achieve this goal, the method proposed in this paper consists of developing a rule-based algorithm that manages the prosumer's Battery Energy Storage System (BESS). The rule-based approach in this type of problem allows for the reduction of computational costs, which is of fundamental importance in contexts where many users will be coordinated simultaneously. This means that the BMS presented in this work could play a vital role in emerging Renewable Energy Communities (RECs). From a general point of view, the method requires an algorithm to process the load and generation profiles of the prosumer for the following three days, together with the hourly price curve. The output is a battery scheduling plan for the timeframe, which is updated every hour. In this paper, the algorithm is validated in terms of economic performance achieved and computational times on two experimental datasets with different scenarios characterized by real productions and loads of prosumers for over a year. The annual economic results are presented in this work, and the proposed rule-based approach is compared with a linear programming optimization algorithm. The comparison highlights similar performance in terms of economic revenue, but the rule-based approach guarantees 30 times lower processing time.

Keywords: battery management system; rule-based optimization; linear programming optimization; smart grids

Citation: Becchi, L.; Belloni, E.; Bindi, M.; Intravaia, M.; Grasso, F.; Lozito, G.M.; Piccirilli, M.C. A Computationally Efficient Rule-Based Scheduling Algorithm for Battery Energy Storage Systems. *Sustainability* **2024**, *16*, 10313. https://doi.org/10.3390/su162310313

Academic Editor: Antonio Caggiano

Received: 11 October 2024
Revised: 22 November 2024
Accepted: 23 November 2024
Published: 25 November 2024

1. Introduction

The evolution of the electricity grid is one of the most profound technological changes in the 21st century. Traditionally, electricity production has been centralized in large power plants, such as coal, gas, nuclear, or hydroelectric plants, located far from the point of consumption. The energy produced in these plants is supplied to end users through High Voltage (HV) and Medium Voltage (MV) transmission lines, as well as Low Voltage (LV) distribution networks. Generally, domestic users and small industries have a low voltage Point Of Delivery (POD), while large industrial users are connected to the MV network with dedicated secondary substations. However, this centralized model is evolving rapidly due to a combination of new technologies, environmental considerations, and the growing demand for electricity. One of the most important trends in many National Electricity

Systems is the transition from centralized generation to Distributed Generation (DG). Unlike large power plants, DG involves small-scale power generation closer to where electricity is consumed [1]. Solar panels on residential rooftops, wind turbines in local communities, and small biomass plants are examples of distributed generation [2]. This transition is driven by the decreasing costs of renewable energy technologies, the desire for energy independence, and political incentives to reduce greenhouse gas emissions. At the same time, the electrification of various sectors, particularly transport through the rise of electric vehicles (EVs), is placing new demands on the electricity grid [3–5]. Electric vehicles require a significant amount of energy for charging, and their widespread adoption is expected to substantially increase electricity demand in the coming years. This increasing load on the system comes at a time when the grid must also accommodate the variability of renewable energy sources, such as solar and wind, which produce energy intermittently depending on weather conditions.

To manage these changes, the role of smart grids and intelligent control systems has become increasingly important [6,7]. This paper proposes a rule-based algorithm capable of managing energy flows between an electricity grid and a prosumer equipped with a photovoltaic system. The proposed method involves scheduling the storage system in synergy with information on the energy price and production/consumption curves. In the near future, smart grids will use digital technology to monitor and manage the flow of electricity in real time, improving efficiency [8–10], reliability [11–13], and flexibility [14–16]. In this sense, the introduction of artificial intelligence algorithms and optimization methods is fundamental in many different sectors. In [8], for example, a great combination of Kernel Principal Component Analysis (KPCA) for feature extraction and an Improved Sparrow Search Algorithm (ISSA) was shown to optimize a Kernel Extreme Learning Machine (KELM) model. In [11], the problem of improving the power output of thermoelectric generators for automotive exhaust heat recovery is addressed, and the key parameters are optimized using an Improved Whale Optimization Algorithm (IWOA). These optimization algorithms fall into a category of very powerful methods from a performance point of view and can be evaluated in the future also for the problem addressed in this paper. However, given priority to the reduction of computational costs, in this work, a rule-based approach is proposed and compared with one of the lightest optimization methods to implement from the point of view of processing time. Likewise, the artificial intelligence algorithms presented in [12–16] represent possible methods to improve the approach proposed in this article and will be taken into consideration in the future to introduce prediction errors in the definition of production/consumption curves. Therefore, by introducing new digital technologies, the integration of distributed energy resources, including the generation and storage of renewable sources, can be facilitated, and the balance between supply and demand can be organized more effectively. A key component of the smart grid is the concept of Demand Response Management (DRM), which involves encouraging consumers to adjust their electricity usage patterns, especially during peak demand periods, through dynamic pricing or automated control systems.

In this context of great transformations, Renewable Energy Communities (RECs) have emerged as a potential solution both to increase local energy self-sufficiency and to improve the overall performance of the electricity grid [17]. These communities are groups of energy consumers, prosumers (those who produce and consume energy), and local energy producers who collaborate to generate, store, and share energy within a defined area [18]. From a general point of view, energy communities leverage local renewable energy sources, such as solar panels and wind turbines, to meet the energy needs of their members. They can also include energy storage systems and electric vehicle charging infrastructure, allowing members to maximize the use of locally generated clean energy. Energy communities also have the potential to reduce energy losses in the distribution network. Indeed, in a traditional centralized system, electricity is transmitted over long distances from power plants to consumers, introducing losses due to the Joule effect. In contrast, energy communities, with their localized generation and consumption, reduce the distance needed for electricity to travel, thus minimizing these losses. Furthermore, by producing energy closer to the point of consumption, they can reduce congestion in the distribution network, easing the pressure on substations and transformers. One of the key aspects of energy communities is their potential to improve grid stability. As more and more renewable energy is integrated into the grid, maintaining the balance between supply and demand becomes increasingly difficult due to the intermittent nature of solar and wind energy. Energy communities, through their local generation and storage capabilities, can provide flexibility to the grid by adapting their consumption and generation patterns based on grid conditions. For example, during periods of high solar production, energy communities can store excess energy in batteries for later use, while during periods of peak demand, they can reduce consumption or even feed the stored energy back into the grid. However, to fully realize these benefits, the control and optimization of energy communities are critical [19].

In some applications of RECs, rule-based approaches are increasingly relevant when compared to metaheuristic or heavy optimization techniques [20–22]. Rule-based systems provide a way to address complex systems with low computational overhead, thereby enabling faster decision-making. Unlike optimization or heuristic approaches, which often require iterative calculations or extensive parameter tuning, rule-based systems rely on predefined rules and logical conditions that can be executed quickly. This reduction in computational load is particularly beneficial in time-critical scenarios, where rapid adjustments in response to real-time data, such as energy demand or changes in production, are essential. Additionally, rule-based methods can offer greater transparency, as they are generally easier to interpret and validate than empirical or black-box optimization techniques. In energy conversion systems, this transparency supports better maintenance and troubleshooting. This advantage is particularly valuable for complex infrastructures, such as those within a smart grid or renewable energy grid, where multiple decentralized actors interact [23]. However, a possible limitation of the rule-based approach in energy management, or any decision-making system, is its reliance on predefined rules that require complete coverage of possible scenarios within the environment. When key contextual factors change, rule-based systems may lack the flexibility to adapt seamlessly. Furthermore, the suboptimal nature of this approach can introduce a loss of accuracy that must be evaluated by the designer in accordance with computational savings. In this scenario, both academic research and engineering applications are moving in different directions, considering rule-based or optimization methods, or hybrid versions of both. Managing RECs with distributed energy storage systems, for example, is a very challenging topic, and many different methods have been developed in recent years. A complete review of these techniques is presented in [24], where the fundamental characteristics of the hybrid approaches called "rule-based optimization" also emerge. In the context of rule-based strategies, ref. [25] presents a general approach to enable residential communities to share solar energy and coordinate distributed energy storage within a specific sharing economy model. Similarly, [26,27] introduces a two-stage management strategy aimed at optimal operation and billing for renewable energy virtual communities. Interesting results on optimization methods for RECs appear in [28,29], where a strategy for scheduling energy storage while maximizing economic gains and minimizing operating costs throughout the year is presented. The characteristics of network management from technical and economic points of view are fundamental to the development of these models; a complete overview can be found in [30]. In particular, the application proposed in [31] examines a small-scale REC based in Italy, incorporating photovoltaic systems, battery energy storage systems, and controllable loads within the scope of current Italian energy policies. From a general point of view, all these methods could help energy communities participate in demand response programs in the future, where they adapt their consumption patterns in response to signals from the grid, such as price fluctuations or requests to reduce demand during peak times.

Starting from these assumptions, the main objective of this paper is to propose a rule-based approach for developing a Battery Management System (BMS) capable of achieving performance comparable to that of other optimization methods. In particular, this work focuses on a single grid-connected prosumer and aims to optimize its energy flows while ensuring the lowest possible processing time. The main idea is to develop a fast rule-based algorithm that is easily scalable to manage many prosumers connected to the same portion of the distribution network, to the same microgrid, or even to the same REC [32]. In fact, as previously mentioned, one of the main problems of approaches based on optimization algorithms is the possibility of finding the optimal solution when a large number of users are involved. Starting from these considerations, the main idea is to develop a hierarchical control method in which a central entity provides hourly energy prices and production/consumption forecasts to each BMS. The latter can quickly define the prosumer's strategy by taking into account battery degradation and consumption habits. This paper presents the final part of this control chain, i.e., a series of rules that optimize the action of a single prosumer. The results obtained not only provide the opportunity to implement a unified strategy within RECs or microgrids, but also offer a strong foundation for enhancing battery management for individual users. Moreover, the use of low-computational-cost algorithms is increasingly seen as a key factor in improving energy efficiency and promoting sustainability. As the demand for real-time data processing and optimization grows, particularly in the management of decentralized energy resources, the computational load becomes a significant consideration. Power-intensive algorithms can lead to increased power consumption in data centers and devices, indirectly contributing to the carbon footprint of what should be a sustainable energy system [33,34]. Efficiently managing energy production, storage, and distribution requires real-time analysis of data from various sources, including solar panels, wind turbines, and energy storage systems. Low-cost algorithms ensure that these data can be processed quickly without excessive computational resources, enabling smarter decision-making and more efficient use of energy. This approach supports the integration of renewable energy sources, improves grid stability, and maximizes the benefits of clean energy. Therefore, the move to low-computational-cost algorithms is not just a technical improvement; it is a step forward towards achieving a more sustainable and resilient energy ecosystem [35,36].

To better understand the control strategy developed in this work, it is necessary to introduce some general and specific considerations. First of all, note that the load and production curves used to define the prosumer's battery actions are considered perfect predictions, i.e., the scenario hypothesized to define the strategy is exactly what then occurs. As regards the daily energy price curve, this is considered to follow the rules of the day-ahead electricity market. Therefore, using these three inputs, the BMS programs 72 successive actions for the battery, one for each hour. The strategy is then updated with a fixed time step of 1 h. This choice is due to the fact that the proposed BMS could be used in emerging energy communities in Italy. In fact, these new entities, according to the rules introduced by Legislative Decree 414/2023, obtain an economic incentive for the energy collectively self-consumed every hour. Therefore, the objective of the RECs is to keep the energy injected into the grid and the energy consumed the same on an hourly basis. The use of perfect forecasts and the absence of a battery degradation model allow this first phase to evaluate in detail only the performance of the control algorithm compared to other optimization strategies proposed in the literature. In this work, a comparison with a standard Linear Programming (LP) optimization technique [37] is presented, but in the future, the discussion could be extended to other methods.

For example, in the optimization-based methods proposed in [38–40], the operation of energy storage systems, electric vehicle chargers, and other flexible loads can be coordinated to minimize energy costs while ensuring that the energy community remains self-sufficient. These approaches can also help balance energy flows within the community, reduce the need for energy imports from the grid, and minimize the risk of overloading the distribution network [41]. One of the most common methods for optimization is Model Predictive

Control (MPC), in which a mathematical model of the energy community is used to predict future energy generation, consumption, and prices over a given time horizon [42,43]. MPC is particularly useful in managing the intermittent nature of renewable energy sources, as it enables proactive decision-making based on forecasts [44,45]. An in-depth review of the advantages and disadvantages of using MPC is provided in Table II of [46]. In general, it can be said that one of the main challenges related to the use of MPC in the management of energy communities is its high computational demand, especially when optimizing over long time horizons or dealing with multiple prosumers and energy assets. This complexity can lead to slower decision-making, which is problematic for real-time applications where fast response times are crucial. This problem is also common to other optimization techniques, which pushes research towards increasingly high-performance algorithms [47]. For example, the study presented in [48] offers a tool to assist Multi-objective Optimization (MO) of solar energy allocation. In fact, specific genetic algorithms (GA) are used to reduce the search space and simplify the constraints. Furthermore, among the most currently used solutions, there are certainly LP or Mixed Integer Linear Programming algorithms (MILP) [49–51]. For example, in [52], an energy integration system called Smart Hybrid Renewable Energy for Communities (SHREC) is proposed. The system addresses both the thermal (heating and cooling) and electricity markets at a large community scale, emphasizing their interaction by leveraging Renewable Energy Sources (RES), Combined Heat and Power (CHP) systems, and energy storage solutions. A planning model based on CHP is developed for the SHREC system, and an LP algorithm is used to optimize energy management over a weekly period. Shifting the focus to storage systems, in [53] the BESS (Battery Energy Storage System) control strategy is composed of three different modules: (i) a machine learning-based forecasting algorithm that provides a one-day-ahead projection for microgrid loads and photovoltaic generation, using historical data sets and weather forecasts; (ii) a MILP algorithm that optimizes the BESS scheduling for the minimum operational costs of the REC; and (iii) a decision tree algorithm running at the intra-hour level, with 1-min time steps and with real load and PV (photovoltaic) generation measurements governing the real-time BESS scheduling.

A detailed description of the hierarchical structure in which the BMS proposed in this work can be used is presented in [54], although in that case, the focus is on a centralized community battery. A similar structure is proposed in [55], where homes compete for the cheapest community-wide renewable energy, while an aggregator minimizes the community's total electricity bill.

Finally, compared to the works present in the literature, this paper provides the following contributions:

- It offers a BMS for a single networked prosumer that can function both autonomously and in a hierarchical structure with a central controller;
- The proposed control rules are easily adaptable to different contexts, both from the point of view of prices and production/consumption;
- The performance of the BMS is comparable to that of one of the most commonly used optimization methods, guaranteeing significant savings in terms of the computational cost and strategy processing time.

This manuscript is organized as follows: Section 2.1 introduces the necessary formalism and notation used throughout the paper, together with some preliminary considerations and hypotheses defining the proposed case study; Section 2.2 defines the LP benchmark used to evaluate the performance of our algorithm, which is presented in Section 2.3; Section 2.4 illustrates the datasets used for testing the scheduling algorithms; Section 3 presents the results of the experimentation, comparing the performance of rule-based and LP optimizations; and finally, Section 4 draws the conclusions.

2. Materials and Methods

2.1. Notation and Preliminary Hypotheses

Considering an electricity user equipped with a PV system, the power exchange with the electrical grid can be represented, without losing generality, as an alternation of injection intervals and withdrawal intervals, as shown in the example in Figure 1. In the following, we refer to the injection periods (green areas in Figure 1) as positive intervals and the withdrawal periods (red areas in Figure 1) as negative intervals. Let T_S be the control time step in hours, i.e., the time granularity of the actions performed by the BMS, and N_H be the control future horizon, i.e., the number of future actions scheduled by the BMS at each algorithm execution. Thus, the system's future time horizon is $T_H = N_H T_S$. In this study, $T_S = 1$ h and $N_H = 72$, yielding $T_H = 72$ h; however, the proposed energy management approach is generalizable to any T_S and N_H values. Since T_S is equal to one hour, we consider the hourly energy exchange with the power grid. As an example, Figure 2 shows the hourly energy exchange corresponding to the power curve in Figure 1. The hourly energy exchange is, therefore, represented as an array $\overline{E}$ of length N_H, with values E_t being the energy exchanged in the t-th hour, $t = 1, \ldots, N_H$.

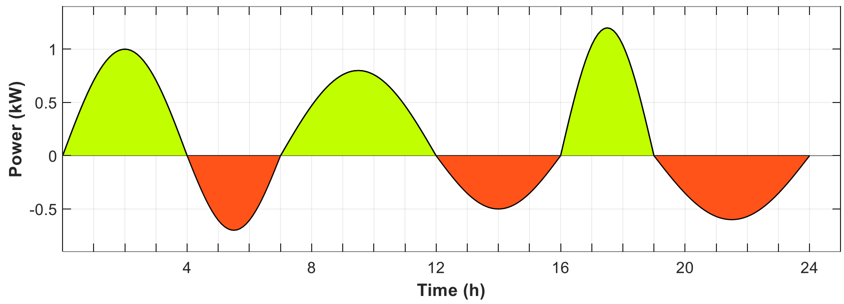

Figure 1. Example of 24 h profile representing the power exchange with the electrical grid for a domestic prosumer. The green areas represent power injections from the user into the grid (positive intervals), while in the red periods, the user takes power from the grid (negative intervals).

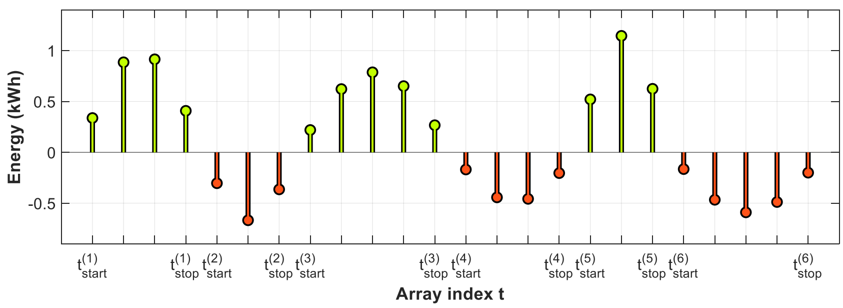

Figure 2. Hourly energy exchange with the electrical grid for a domestic prosumer (corresponding to the example in Figure 1). Each bar represents the energy injected into (or taken from) the grid during that hour.

The energy exchange sequence $\overline{E}$ is also composed of alternating positive and negative intervals. We denote with N_I the total number of positive and negative intervals, and we indicate the intervals as I_j, $j = 1, \ldots, N_I$. Moreover, we denote with $\boldsymbol{I_H}$ the union of all the intervals:

$$\boldsymbol{I_H} = \bigcup_{j=1}^{N_I} I_j \tag{1}$$

For each interval, we define

- the start index $t^{(j)}_{start}$, with $j = 1, \ldots, N_I$, as the position of the first element of the j-th interval in the array $\overline{E}$.

- the stop index $t_{stop}^{(j)}$, with $j = 1, \ldots, N_I$, as the position of the last element of the j-th interval in the array $\overline{E}$.
- the interval energy $E_{tot,j}$, with $j = 1, \ldots, N_I$, as the total energy exchanged in the j-th interval. $E_{tot,j}$ is computed as

$$E_{tot,j} = \sum_{t=t_{start}^{(j)}}^{t_{stop}^{(j)}} E_t \tag{2}$$

Conventionally, energy is considered positive when injected into the grid and negative when withdrawn from the grid.

Note that $t_{start}^{(1)}$ and $t_{stop}^{(N_I)}$ correspond respectively to the array indices 1 and N_H. Using the introduced notation, each generic sequence $\overline{E}$ of N_H samples can be mapped in a matrix containing the $t_{start}^{(j)}$ and $t_{stop}^{(j)}$ indices, and the interval energies $E_{tot,j}$. Table 1 shows the mapping matrix obtained for the example sequence shown in Figure 2. In this case, $N_I = 6$, and therefore, the mapping matrix has 18 elements.

Table 1. Mapping matrix resulting from the sequence in Figure 2.

	j = 1	**j = 2**	**j=3**	**j = 4**	**j = 5**	**j = 6**
$t_{start}^{(j)}$	1	5	8	13	17	20
$t_{stop}^{(j)}$	4	7	12	16	19	24
$E_{tot,j}$ (kWh)	2.544	−1.336	2.547	−1.273	2.289	−1.909

As the BMS objective is to maximize the economic benefits based on the trend of the electricity market, we introduce the following important hypothesis: in each considered control horizon of N_H actions, the minimum purchase price is higher than the maximum selling price. Such condition can be written as

$$\min_{t \in \boldsymbol{I_H}} C_t^{(p)} > \max_{t \in \boldsymbol{I_H}} C_t^{(s)} \quad \forall \boldsymbol{I_H} \tag{3}$$

where $C_t^{(p)}$ and $C_t^{(s)}$ are respectively the purchase price and the selling price, $t = 1, \ldots, N_H$. This condition implies that it is always more convenient to store the excess production in the battery if needed for future usage in negative intervals, instead of selling the overproduced energy and buying it back later. Such an assumption usually holds, even though in recent years, mainly due to the consequences of COVID-19, there have been cases where the high instability of the energy market has led to a violation of this hypothesis. In this work, we do not take into account such exceptions. To help visualize the condition expressed by inequality (3), Figures 3 and 4 show, respectively, a situation where the hypothesis is respected and a situation in which it is violated.

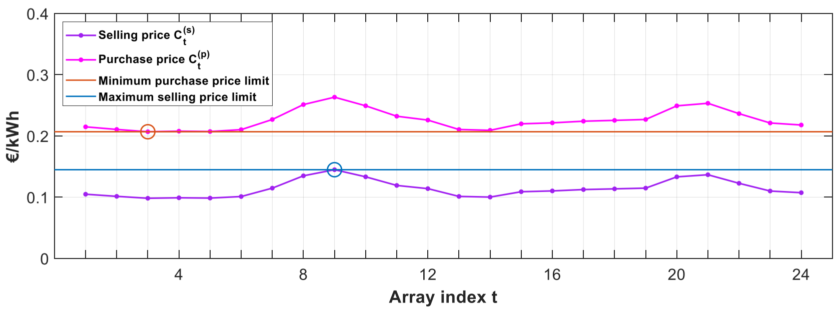

Figure 3. Example of selling price and purchase price trends respecting condition (3).

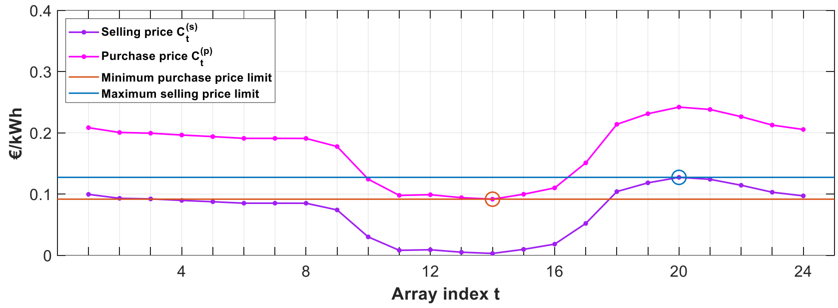

Figure 4. Example of selling price and purchase price trends violating condition (3). In this case, the minimum purchase price (red line) is below the maximum selling price (blue line).

In this study, we refer to the Italian framework and therefore consider the following energy prices, according to the Italian regulation of the energy market and to what was established by the GSE (Gestore dei Servizi Energetici, i.e., the Italian energy services manager):

- The selling price $C_t^{(s)}$ is set equal to the PUN (Prezzo Unico Nazionale).
- The purchase price is calculated as $C_t^{(p)} = 1.21C_t^{(s)} + 0.088$ €/kWh, where the second constant term accounts for taxes and system charges.

Before introducing the LP cost function and constraints, some additional definitions are needed:

- $\overline{E}_0$ is the original sequence $\overline{E}$ (i.e., the energy exchange with the power grid) of length N_H, without the contributions from the BESS. The elements of $\overline{E}_0$ are $E_{0,t}$, $t = 1, \ldots, N_H$.
- $\overline{e}_B$ is the sequence of actions on the energy storage scheduled for the next N_H time steps, i.e., is an array of length N_H containing the energy exchanged with the storage. The elements of $\overline{e}_B$ are $e_{B,t}$, $t = 1, \ldots, N_H$. Conventionally, $\overline{e}_B$ is positive when the energy is stored in the battery and negative when the energy is drawn from the battery.
- $\overline{E}_B$ is the sequence $\overline{E}_0$ considering the contributions of $\overline{e}_B$, as established by the scheduling algorithm. In other terms, the actions $\overline{e}_B$ modify the original energy exchange with the grid vector $\overline{E}_0$, yielding a new energy exchange vector $\overline{E}_B$. The elements of $\overline{E}_B$ are $E_{B,t}$, $t = 1, \ldots, N_H$. As such, it holds:

$$E_{B,t} = E_{0,t} - e_{B,t} \quad t = 1, \ldots, N_H \tag{4}$$

or, in vectorial notation:

$$\overline{E}_B = \overline{E}_0 - \overline{e}_B \tag{5}$$

Note that, to ease readability, quantities indicated with capital "E" refer to energy exchanges with the electrical grid, while quantities indicated with lowercase "e" refer to energy exchanges with the BESS.

- We denote, respectively, with $\boldsymbol{I_{neg}}$ and $\boldsymbol{I_{pos}}$ the set of negative intervals and the set of positive intervals. $\boldsymbol{I_H}$ is defined as in Equation (1). Therefore, it also holds: $\boldsymbol{I_H} = \boldsymbol{I_{neg}} \cup \boldsymbol{I_{pos}}$.
- The energy price array $\overline{C}$, with elements C_t, $t = 1, \ldots, N_H$, is defined as follows:

$$\begin{cases} C_t = C_t^{(p)} & \text{if } t \in \boldsymbol{I_{neg}} \\ C_t = C_t^{(s)} & \text{if } t \in \boldsymbol{I_{pos}} \end{cases} \tag{6}$$

Figure 5 shows how the $\overline{C}$ array is derived from purchase and selling prices, considering, as an example, the intervals in Figure 2.

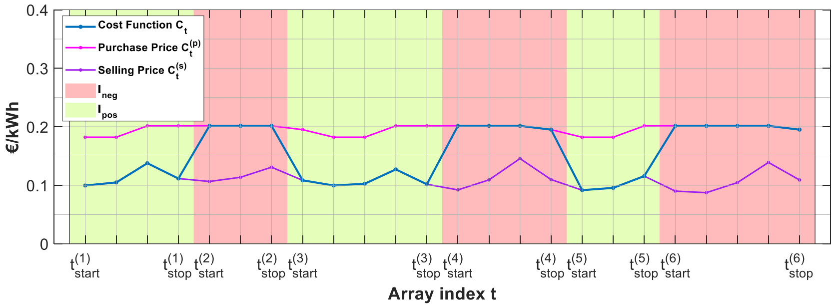

Figure 5. Example of derivation of the energy price array $\overline{C}$, given the energy profile in Figure 2.

- SOC_j, $j = 1, \ldots, N_I$, represents the BESS charge level at the end of the j-th interval; SOC_M is the maximum battery charge level; SOC_m is the minimum battery charge level. As such, the maximum possible energy exchange with the storage at each control time step is $e_{B,\text{full}} = SOC_M - SOC_m$.

2.2. Linear Programming Benchmark Definition

Given the premises of the previous section, the LP cost function is formulated as

$$\begin{gathered} \min_{E_{B,t}} \left(-\sum_{t=1}^{N_H} E_{B,t} C_t \right) \\ \textbf{subject to} \\ \gamma_1, \gamma_2 \end{gathered} \tag{7}$$

γ_1 and γ_2 are the problem constraints, as defined in the following. The first constraint γ_1 establishes the lower and upper boundaries for $\overline{E}_B$ as

$$\min(E_{0,t}, 0) \leq E_{B,t} \leq \max(E_{0,t}, 0) \quad \forall t \in \boldsymbol{I_H} \tag{8}$$

Such a constraint implies that the battery can never exchange energy directly with the grid. This entails, at the same time, the impossibility of changing a positive interval into a negative one (and vice versa) by selling or buying additional energy. Figure 6 shows the limits defined in (8) for the energy profile shown in Figure 2.

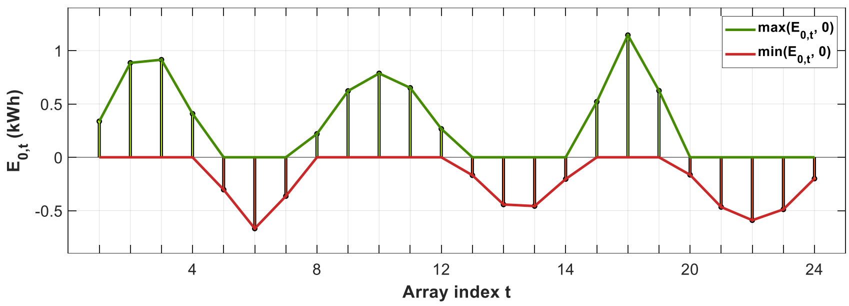

Figure 6. Visualization of the limits imposed by the constraint (8).

Secondly, we define, for each interval, a γ_2 constraint as a linear inequality to limit the battery usage so that it always operates under the safe operating conditions (in terms of charge level) recommended by the manufacturer. As such, γ_2 is a set of linear inequality constraints, one for each interval. This is achieved by ensuring that the battery can never overcharge (over the SOC_M limit) in a positive interval or be depleted completely (under the SOC_m limit) in a negative interval. Therefore, we can express the γ_2 a constraint for the j-th interval as

$$\begin{cases} SOC_j \leq SOC_M & \text{if } I_j \subseteq \boldsymbol{I_{pos}} \\ SOC_j \geq SOC_m & \text{if } I_j \subseteq \boldsymbol{I_{neg}} \end{cases} \tag{9}$$

$$SOC_j = SOC_{j-1} + \sum_{t=t_{start}^{(j)}}^{t_{stop}^{(j)}} e_{B,t}, \quad j = 1, \ldots, N_I \tag{10}$$

Note that SOC_j for $j = 0$ is the battery state of charge at the beginning of the scheduling sequence, determined by previously performed actions. It is possible to express the generic SOC_j in terms of SOC_0 by recursively developing Equation (10), yielding:

$$SOC_j = SOC_0 + \sum_{t=t_{start}^{(1)}}^{t_{stop}^{(j)}} e_{B,t}\,, \quad j = 1, \ldots, N_I \tag{11}$$

Rewriting (9) using (11) and also introducing the relationship given by (4), we obtain

$$\begin{cases} SOC_0 + \sum\limits_{t=t_{start}^{(1)}}^{t_{stop}^{(j)}} E_{0,t} - \sum\limits_{t=t_{start}^{(1)}}^{t_{stop}^{(j)}} E_{B,t} \leq SOC_M \text{ if } I_j \subseteq \boldsymbol{I_{pos}} \\ SOC_0 + \sum\limits_{t=t_{start}^{(1)}}^{t_{stop}^{(j)}} E_{0,t} - \sum\limits_{t=t_{start}^{(1)}}^{t_{stop}^{(j)}} E_{B,t} \geq SOC_m \text{ if } I_j \subseteq \boldsymbol{I_{neg}} \end{cases} \quad j = 1, \ldots, N_I \tag{12}$$

Rearranging the terms in (12) yields the following expression for the γ_2 constraints:

$$\begin{cases} \sum\limits_{t=t_{start}^{(1)}}^{t_{stop}^{(j)}} E_{B,t} \geq SOC_0 - SOC_M + \sum\limits_{t=t_{start}^{(1)}}^{t_{stop}^{(j)}} E_{0,t} \text{ if } I_j \subseteq \boldsymbol{I_{pos}} \\ \sum\limits_{t=t_{start}^{(1)}}^{t_{stop}^{(j)}} E_{B,t} \leq SOC_0 - SOC_m + \sum\limits_{t=t_{start}^{(1)}}^{t_{stop}^{(j)}} E_{0,t} \text{ if } I_j \subseteq \boldsymbol{I_{neg}} \end{cases} \quad j = 1, \ldots, N_I \tag{13}$$

2.3. Rule-Based Algorithm Definition

In this section, the proposed rule-based approach is introduced. The algorithm is formulated to achieve the same objective expressed by the LP cost function (7), i.e., the maximization of the prosumer revenue derived from the management of the battery. The implemented rule-based algorithm consists of the following three main steps.

Step 1. Determination of the energy possibly requested from the battery and the energy possibly available for storage in the battery in each interval I_j. These quantities are indicated respectively as $\bar{e}_R$ and $\bar{e}_A$, are vectors of size N_I, with elements denoted as $e_{R,j}$ and $e_{A,j}$, and are computed as follows:

$$e_{R,j} = \begin{cases} 0 \text{ if } I_j \subseteq \boldsymbol{I_{pos}} \\ \max\left(E_{tot,j}, -e_{B,\text{full}}\right) \text{ if } I_j \subseteq \boldsymbol{I_{neg}} \end{cases} \quad j = 1, \ldots, N_I \tag{14}$$

$$e_{A,j} = \begin{cases} \min\left(E_{tot,j}, e_{B,\text{full}}\right) \text{ if } I_j \subseteq \boldsymbol{I_{pos}} \\ 0 \text{ if } I_j \subseteq \boldsymbol{I_{neg}} \end{cases} \quad j = 1, \ldots, N_I \tag{15}$$

In a positive interval, the energy request from the battery must be zero, whereas the available energy surplus (and, potentially, storable in the battery) is equal to the quantity $E_{tot,j}$ defined in Equation (2). The upper limit of $E_{tot,j}$ is the full battery capacity $e_{B,\text{full}}$. Similarly, in a negative interval, the energy request from the battery is equal to $E_{tot,j}$, with a lower limit of $e_{B,\text{full}}$, while the available energy is zero. Note that, coherently with the convention adopted for $e_{B,t}$, $e_{R,j}$ is always nonpositive, as it represents energy that may be drawn from the battery, while $e_{A,j}$ is nonnegative, indicating energy that may be stored in the battery. The vectors $\bar{e}_R$ and $\bar{e}_A$ are combined into a single vector $\bar{e}_{R/A}$ as follows:

$$e_{R/A,j} = e_{R,j} + e_{A,j} = \begin{cases} \min\left(E_{tot,j}, e_{B,\text{full}}\right) & \text{if} \quad I_j \subseteq \boldsymbol{I_{pos}} \\ \max\left(E_{tot,j}, -e_{B,\text{full}}\right) & \text{if} \quad I_j \subseteq \boldsymbol{I_{neg}} \end{cases} \quad j = 1, \ldots, N_I \tag{16}$$

A detailed flowchart of the first step of the algorithm is shown in Figure 7.

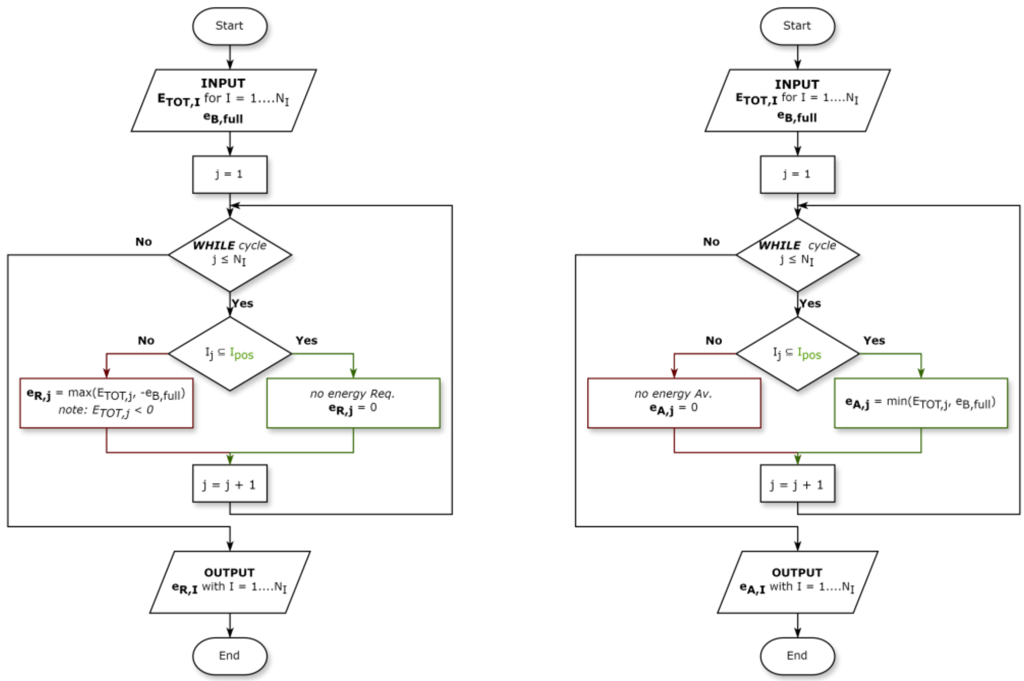

Figure 7. Flowchart of the first step of the rule-based algorithm. The **left** and **right** branches illustrate, respectively, the procedure to determine $\bar{e}_R$ and $\bar{e}_A$.

Step 2. Determination of the target energy amount that the system would need to move from or to the battery at each interval. We denote this quantity as $\bar{e}_{target}$, having elements $e_{target,j}$, $j = 1, \ldots, N_I$. We also introduce the vector $\bar{e}_R^{(next)}$, with elements $e_{R,j}^{(next)}$, $j = 1, \ldots, N_I$, containing, for each interval, the cumulative unsatisfied energy request remaining from all the future intervals. The calculation of these quantities is performed starting from the last interval I_{N_I} and proceeding backward, as illustrated in the flowchart in Figure 8. In this way, the algorithm can correctly compute $\bar{e}_R^{(next)}$ for all the previous intervals. For the last interval, we set

$$e_{R,N_I}^{(next)} = 0$$

$$e_{target,N_I} = \begin{cases} \max\left(e_{R/A,N_I}, E_{pos}^{(avg)}\right) & \text{if} \quad I_{N_I} \subseteq \boldsymbol{I_{pos}} \\ \min\left(e_{R/A,N_I}, E_{neg}^{(avg)}\right) & \text{if} \quad I_{N_I} \subseteq \boldsymbol{I_{neg}} \end{cases} \tag{17}$$

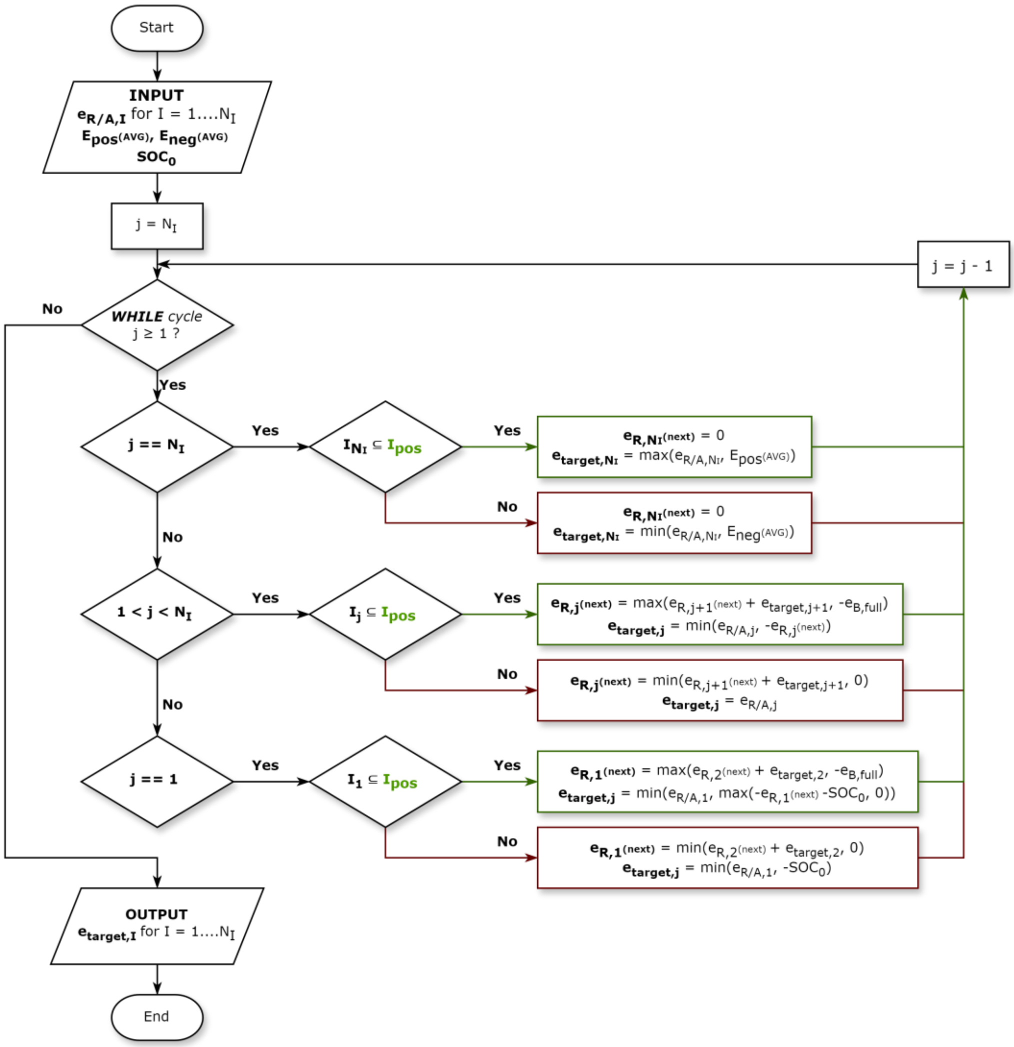

Figure 8. Flowchart of the second step of the rule-based algorithm.

Equation (17) is established based on the following assumptions:

- $e_{R,N_I}^{(next)}$, i.e., the unsatisfied energy request from time instants beyond the system's future time horizon T_H, is set to zero.
- If $I_{N_I} \subseteq \boldsymbol{I_{pos}}$, e_{target,N_I} is forced to be at least $E_{pos}^{(avg)}$, which is the average energy surplus in the positive intervals computed using the available past data. This is to consider that moving the algorithm horizon forward, more energy to be stored can be available if the positive interval is extended further.
- If $I_{N_I} \subseteq \boldsymbol{I_{neg}}$, e_{target,N_I} is forced to be at maximum $E_{neg}^{(avg)}$, which is the average energy deficiency in the negative intervals computed on the available past data. Similar to the previous point, this assumption takes into account that the last negative interval may extend further and require more energy.

For the other intervals, $e_{target,j}$ and $e_{R,j}^{(next)}$ are computed as follows:

$$
\begin{aligned}
e_{R,j}^{(next)} &= \begin{cases} \max\left(e_{R,j+1}^{(next)} + e_{target,j+1}, -e_{B,\text{full}}\right) & \text{if } \ I_j \subseteq \boldsymbol{I_{pos}} \\ \min\left(e_{R,j+1}^{(next)} + e_{target,j+1}, 0\right) & \text{if } \ I_j \subseteq \boldsymbol{I_{neg}} \end{cases} \qquad j = 2, \ldots, N_I - 1 \\
e_{target,j} &= \begin{cases} \min\left(e_{R/A,j}, -e_{R,j}^{(next)}\right) & \text{if } \ I_{N_I} \subseteq \boldsymbol{I_{pos}} \\ e_{R/A,j} & \text{if } \ I_{N_I} \subseteq \boldsymbol{I_{neg}} \end{cases} \qquad j = 2, \ldots, N_I - 1
\end{aligned} \tag{18}
$$

Finally, for the first interval I_1, the initial state of charge of the battery SOC_0 must be considered:

$$e_{R,1}^{(next)} = \begin{cases} \max\left(e_{R,2}^{(next)} + e_{target,2}, -e_{B,\text{full}}\right) & \text{if} \quad I_1 \subseteq \boldsymbol{I_{pos}} \\ \min\left(e_{R,2}^{(next)} + e_{target,2}, 0\right) & \text{if} \quad I_1 \subseteq \boldsymbol{I_{neg}} \end{cases}$$
$$e_{target,1} = \begin{cases} \min(e_{R/A,1}, \max(-e_{R,1} - SOC_0, 0)) & \text{if} \quad I_1 \subseteq \boldsymbol{I_{pos}} \\ \min\left(e_{R/A,j}, -SOC_0\right) & \text{if} \quad I_1 \subseteq \boldsymbol{I_{neg}} \end{cases} \tag{19}$$

Step 3. Determination of the final battery scheduling $\bar{e}_B$ that the system will try to follow. This is achieved by distributing the quantities $e_{target,j}$, calculated at step 2, inside each interval. Note that, in contrast to step 2, this operation is performed starting from the first interval and proceeding forward. In this way, the computation of $\bar{e}_B$ considers that, in some intervals, it could be impossible to move the whole $e_{target,j}$ due to the battery capacity limits. The criteria to perform the scheduling are as follows:

- In positive intervals, the algorithm schedules the battery recharging by distributing the calculated $e_{target,j}$ among the interval time slots, starting from the time indices corresponding to the lower energy selling price. This is performed iteratively until the entire quantity $e_{target,j}$ is transferred to the battery or until the battery is fully replenished. An example of scheduling in a positive interval, considering a battery capacity of 3 kWh that is initially fully discharged, is shown in Figure 9. In this case, the algorithm identifies the third slot of the interval as the least convenient for selling energy, and therefore, it decides to give priority to that slot for charging the battery. The process is repeated until the desired energy amount ($e_{target,j} = 2.5$ kWh in this example) is stored in the battery at the fourth iteration. The remaining energy is sold to the GSE at the selling price given by C_t.
- In negative intervals, the algorithm schedules the battery discharge by distributing the calculated $e_{target,j}$ among the interval time slots, starting from the time indices characterized by the highest energy purchase price. This is performed iteratively until the entire quantity $e_{target,j}$ is provided by the battery or until the battery is fully depleted. Figure 10 shows an example of scheduling in a negative interval. In this case, the algorithm gives priority to the slot with the highest energy purchase price for drawing energy from the battery. At the fourth iteration, the scheduling procedure ends as the battery is fully depleted. The extra energy need will be covered by buying the energy at the purchase cost given by C_t.

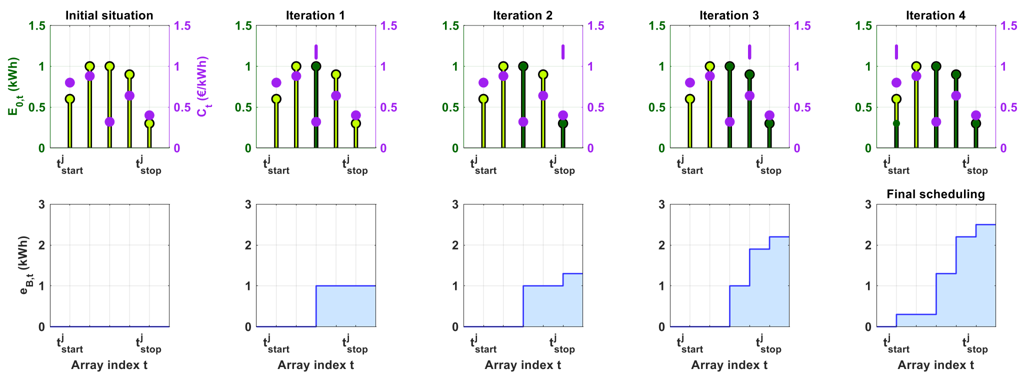

Figure 9. Example of scheduling in a positive interval.

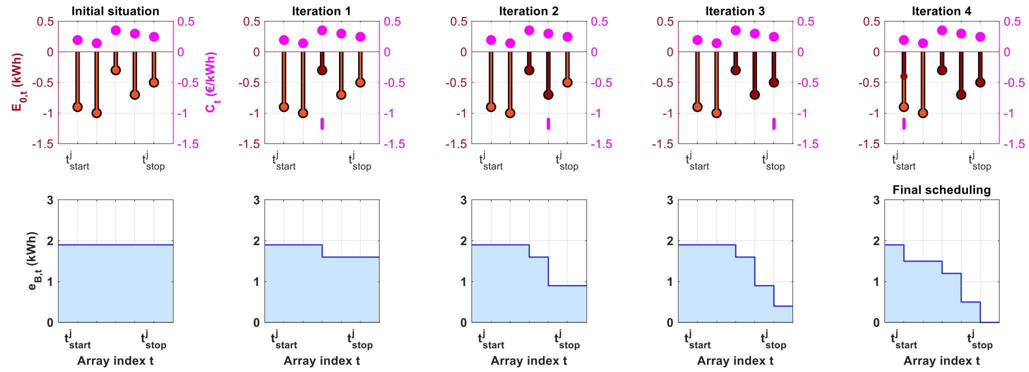

Figure 10. Example of scheduling in a negative interval.

The operations described in this third step are represented visually in the flowcharts shown in Figures 11 and 12. Such flowcharts describe in detail how scheduling for positive and negative intervals is obtained for a given $\bar{e}_{target}$ vector.

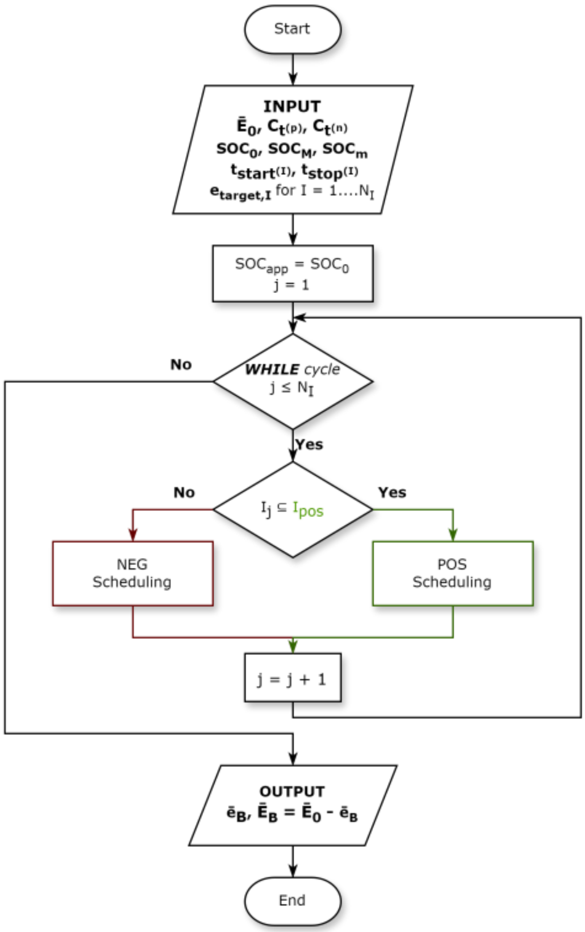

Figure 11. Flowchart of the third step of the rule-based algorithm. The "NEG Scheduling" and "POS Scheduling" blocks are illustrated in Figure 12.

Figure 12. Operations performed in the "NEG Scheduling" block (on the **left**) and "POS Scheduling" block (on the **right**) of Figure 11.

2.4. Datasets

The described LP and rule-based approaches are tested on two datasets containing historical production and consumption data of real prosumers. No user is equipped with a BESS; therefore, the presence of a storage system is hypothesized in the simulation. Additionally, the historical trends of the energy market (i.e., the PUN made available by the GSE) are considered as the reference for the energy price. All data are in an hourly format. The details of these datasets are summarized below:

- Ausgrid [56]: it contains one year (8760 samples per user) of production and consumption data of 126 prosumers. This dataset, indicated as the AUS dataset in the following, is publicly available on the Ausgrid website.
- Planet Smart City [57]: it contains five months of data (around 3550 samples per user) related to 286 users residing in the Milan area in north Italy. These users are actually pure consumers; therefore, production data are artificially added by hypothesizing the PV and BESS sizes (the values are listed below) and using solar irradiation data obtained from PVGIS [58]. This dataset, indicated as the PSC dataset in the following, was provided in the context of a collaboration between the University of Florence and the Planet Smart City company.
- The energy price historical data are available on the GSE website [59]. This study was carried out considering PUN trends extracted from 2020 (stable energy cost around 0.05 €/kWh). In the selected period, the hypothesis given by Equation (3) always holds.

Furthermore, the datasets are augmented by rescaling the consumption and production profiles of each user to have an annual consumption of 3 MWh or 6 MWh and a solar plant size of 3 kW or 6 kW. Additionally, BESS capacities of 6 kWh and 12 kWh are considered. These six options are combined in every possible way, producing eight different scenarios for testing the scheduling algorithms. In the following, the scenarios are indicated by $s = 1, \ldots, 8$. Each scenario comprises 126 "rescaled" users obtained from the AUS dataset and 286 "rescaled" users obtained from the PSC dataset. The dataset is denoted by d.

3. Results

The results of the application of the two scheduling algorithms on the AUS and PSC datasets are presented in this section as a comparison between the two approaches in terms of the computational time and economic benefits received by each user. All the algorithms are implemented in MATLAB R2024a and run on a machine with an Intel Core i9-139000K processor (Santa Clara, CA, USA) and 32 GB RAM.

Both the LP and rule-based algorithms, implemented in a BMS based on a receding horizon approach, are tested on the eight scenarios introduced in Section 2.4. The battery scheduling algorithms are executed once per hour (i.e., per each sample in the datasets), establishing the actions to be taken on the battery for the next N_H hours (72 in this study). Only the effect of the first scheduled action is considered. Then, the algorithm horizon is shifted by an hour in the future, and a new scheduling strategy is developed.

The results of this extensive experimentation are presented in detail in this section. Tables 2 and 3 summarize the results obtained on the PSC dataset and on the AUS dataset. In the two tables, T_{RB} and T_{LP} represent, respectively, the time required by the rule-based algorithm and the LP algorithm to produce a complete 72-h battery scheduling. Considering the LP scheduling as the best possible strategy, $\Delta_{rev,s}$ is the average percentage error made by the rule-based algorithm in terms of economic revenue with respect to the LP in each scenario s. In other terms, $\Delta_{rev,s}$ quantifies the economic loss (average for all users in the scenario) when using the rule-based approach compared to the LP approach, which is considered the gold standard. As such, $\Delta_{rev,s}$ is defined as follows:

$$\Delta_{rev,[i,s]} = \frac{rev_{RB,[i,s]}^{(final)} - rev_{LP,[i,s]}^{(final)}}{rev_{LP,[i,s]}^{(final)}} \cdot 100 \quad (20)$$

$$\Delta_{rev,\ s} = \frac{1}{N_{user}} \sum_{i=1}^{N_{user}} \Delta_{rev,[i,s]} \quad (21)$$

where i is the user index and N_{user} is the number of users, s is the scenario index, $rev_{RB,[i,s]}^{(final)}$ and $rev_{LP,[i,s]}^{(final)}$ are the final economic revenue of rule-based and LP algorithms resulting at the end of the simulation (8760 h for the AUS dataset scenarios, 3550 h for the PSC dataset scenarios) for user i in scenario s. These quantities are calculated in Tables 2 and 3 separately for the two datasets. By definition, $\Delta_{rev,[i,s]}$ is negative if the rule-based algorithm performance is worse than that of the LP algorithm performance.

Table 2. Results on PSC dataset. The values reported below are averaged for all users included in each scenario.

Scenario			T_{RB} (ms)	T_{LP} (ms)	$\Delta_{rev,s}$ (%)
Load (kW)	**PV Size (kW)**	**BESS Size (kW)**			
3	3	6	~20 ms	~720 ms	−1.55
3	3	12			−4.31
3	6	6			−0.71
3	6	12			−1.80
6	3	6			−0.19
6	3	12			−0.53
6	6	6			−0.39
6	6	12			−1.55

Table 3. Results on AUS dataset. The values reported below are averaged on all the users included in each scenario.

Scenario			T_{RB} (ms)	T_{LP} (ms)	$\Delta_{rev,s}$ (%)
Load (kW)	PV Size (kW)	BESS Size (kW)			
3	3	6	~20 ms	~720 ms	−0.02
3	3	12			−4.13
3	6	6			−0.18
3	6	12			−0.54
6	3	6			−0.12
6	3	12			−0.56
6	6	6			−0.004
6	6	12			−1.02

Figure 13 shows on the left the distribution of $\Delta_{rev,[i,s]}$ considering both datasets; on the right, the revenue trend in time, averaged on the users, is reported for each scenario, comparing the two proposed algorithms. Note that the percentage difference between the last points of each couple of curves corresponds to $\Delta_{rev,\ s}$. These results prove that, in terms of economic revenue, the rule-based algorithm, even if reaching a slightly sub-optimal solution, is able to closely approach the performance achieved through LP in all the tested scenarios. However, the rule-based approach provides battery scheduling in a fraction of the time required by the LP algorithm, making our rule-based solution preferable in situations where computational efficiency is critical.

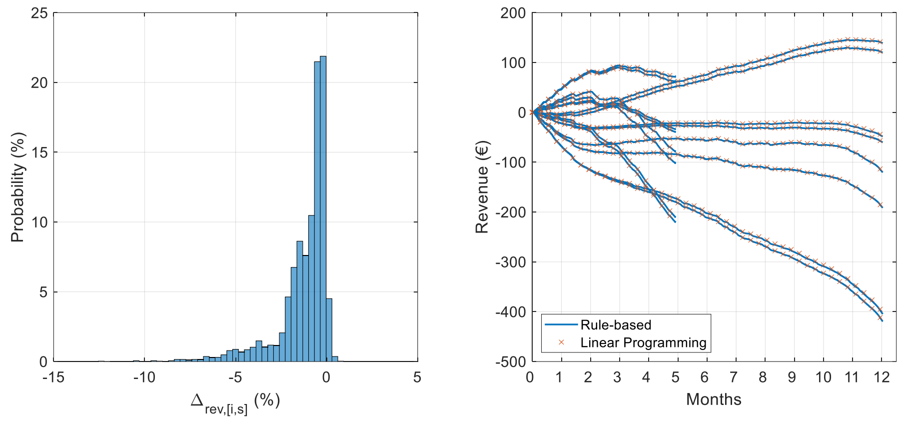

Figure 13. On the **left**: probability distribution of $\Delta_{rev,[i,s]}$ including both datasets; on the **right**: comparison of the average revenue obtained by the users in each scenario when using the LP approach or the rule-based approach. The two curves are visually indistinguishable because the error made by the rule-based algorithm is too small to be appreciated at the scale of the plot.

Information regarding the execution time of the algorithms is particularly interesting from the perspective of the scalability of the management system. As shown in Figure 14, when increasing the number of scheduled actions N_H, for instance, to achieve a finer time granularity of the scheduling, the rule-based approach becomes progressively more clearly preferable to LP in terms of time efficiency, as the computational time does not vary linearly with the length of the scheduled sequence. In Figure 14, this advantage is shown from a graphical point of view, and it is possible to understand how it becomes significant for high values of N_H. For example, for a 1 day schedule with a time interval of 1 min (1440 points), the rule-based algorithm is already over 100 times faster than LP optimization.

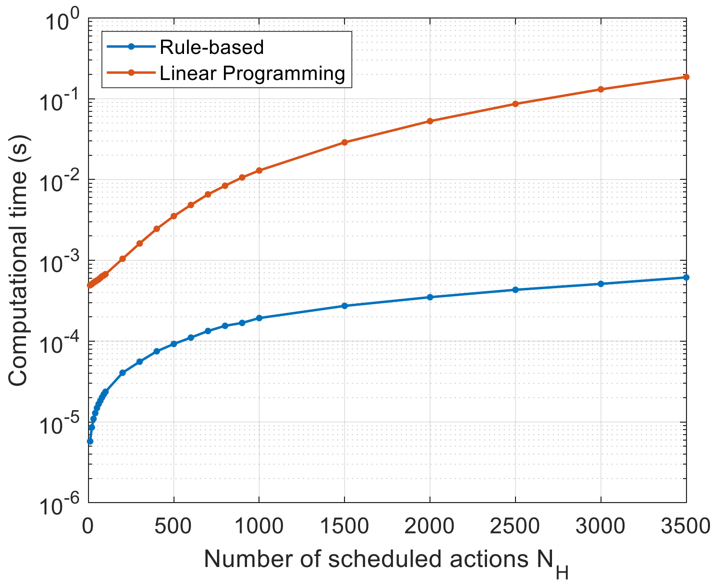

Figure 14. Comparison between the computational time of the rule-based and the LP algorithms for increasing values of N_H.

4. Conclusions

This work mainly focused on the development of a computationally efficient algorithm for managing the energy flows of a grid-connected prosumer with a photovoltaic system and a BESS. The proposed BMS aims to maximize the prosumer's economic gains by optimizing the use, storage, and trading of photovoltaic energy based on market prices and daily production and consumption profiles. The rule-based approach was chosen to achieve lower computational costs in defining the battery scheduling strategy, while maintaining economic revenues comparable to those of other optimization methods. Therefore, this paper proposed a comparison between two different approaches in developing a BMS for a single prosumer: a rule-based approach designed and implemented by the authors and a classical approach based on linear programming optimization. The performances of the two methods are compared under two important assumptions: perfect predictions of the electric load and generation are available for the scheduling time window, and no battery deterioration model is considered. Such simplifications were introduced with the aim of isolating the evaluation of scheduling algorithms from external factors such as forecasting uncertainty.

The results can be summarized in two main points:

i. Both techniques led to extremely similar outcomes in terms of economic revenue, with the LP generally producing slightly better results.
ii. In terms of computational time, the rule-based algorithm is around 30 times faster than its LP counterpart when scheduling 72 future actions on the battery. This difference becomes more relevant by increasing the number of scheduled actions N_H.

These results indicate that the proposed rule-based algorithm is a viable alternative to the more common LP approaches for developing a BMS for a single prosumer equipped with a renewable energy generator and energy storage. While the performance in terms of economic revenue is comparable, the rule-based approach outperforms LP optimization in terms of computational efficiency. This characteristic is fundamental when system scalability is required, such as in the context of energy communities, where hundreds or even thousands of users need to be controlled and coordinated at the same time. Studies have proven that in these scenarios, the most commonly used algorithms, such as MILP, become too complex and thus inapplicable [20]. Rule-based approaches, such as the one proposed in this study, are inherently more suited for implementation in a large-scale management system. Following these considerations, we foresee two main routes for the future development of this work:

- To study the effect of the introduction into the rule-based model of forecasting uncertainty and a battery degradation model. Moreover, the forecasting algorithms should be light enough to be possibly implemented on edge computing devices [60].
- To conceive a higher-level management system that is able to coordinate the single battery management systems based, for example, on the necessities of an energy community (collective self-consumption incentive or ancillary services).

Author Contributions: Conceptualization, L.B., G.M.L. and F.G.; methodology, L.B. and G.M.L.; software, L.B.; validation, L.B., M.B., M.I. and G.M.L.; formal analysis, M.I.; investigation, L.B., E.B., M.I. and G.M.L.; resources, M.B.; data curation, L.B., E.B., M.B. and M.I.; writing—review and editing, L.B., M.B., M.C.P. and M.I.; visualization, L.B. and M.I.; supervision, G.M.L. and F.G.; project administration, G.M.L., M.C.P. and F.G. All authors have read and agreed to the published version of the manuscript.

Funding: This project was funded by the European Union, Next Generation EU, Mission 4, Component 1, CUP J53D23000760006. The authors also acknowledge the financial support of the National Research Center in High-Performance Computing, Big Data and Quantum Computing (https://www.supercomputing-icsc.it/en/icsc-home/, accessed on 1 October 2024) foreseen within Mission 4 (Education and Research) of the "National Recovery and Resilience Plan" (NRRP) that is part of the Next Generation EU (NGEU) program (https://www.italiadomani.gov.it/en/, accessed on 1 October 2024).

Data Availability Statement: The data presented in this study were derived from the following resources available in the public domain: Ausgrid dataset, https://www.ausgrid.com.au/ (accessed on 1 October 2024); Italian energy market trends, https://www.gse.it/ (accessed on 1 October 2024); solar irradiation data, https://joint-research-centre.ec.europa.eu/photovoltaic-geographical-information-system-pvgis_en (accessed on 1 October 2024). The Planet Smart City dataset is not readily available as it is part of privacy-sensitive material provided by company PLANET IDEA S.r.l.

Acknowledgments: The authors acknowledge the support of company PLANET IDEA S.r.l. for the concession in the use of data.

Conflicts of Interest: The authors declare no conflicts of interest.

References

1. Saad, O.; Abdeljebbar, C. Historical Literature Review of Optimal Placement of Electrical Devices in Power Systems: Critical Analysis of Renewable Distributed Generation Efforts. *IEEE Syst. J.* **2021**, *15*, 3820–3831. [CrossRef]
2. Brumana, G.; Ghirardi, E.; Franchini, G. Comparison of Different Power Generation Mixes for High Penetration of Renewables. *Sustainability* **2024**, *16*, 8435. [CrossRef]
3. Zakaria, H.; Hamid, M.; Abdellatif, E.M.; Imane, A. Recent Advancements and Developments for Electric Vehicle Technology. In Proceedings of the 2019 International Conference of Computer Science and Renewable Energies (ICCSRE), Agadir, Morocco, 22–24 July 2019; pp. 1–6. [CrossRef]
4. Tambunan, H.B. Electric Vehicle Integration into Electrical Power System: A Bibliometric Review. In Proceedings of the 2022 International Conference on Technology and Policy in Energy and Electric Power (ICT-PEP), Jakarta, Indonesia, 18–20 October 2022; pp. 65–70. [CrossRef]
5. Yan, Q.; Wang, Z.; Xing, L.; Zhu, C. Optimal Economic Analysis of Battery Energy Storage System Integrated with Electric Vehicles for Voltage Regulation in Photovoltaics Connected Distribution System. *Sustainability* **2024**, *16*, 8497. [CrossRef]
6. Blfgeh, A.; Alkhudhayr, H. A Machine Learning-Based Sustainable Energy Management of Wind Farms Using Bayesian Recurrent Neural Network. *Sustainability* **2024**, *16*, 8426. [CrossRef]
7. Andreotti, D.; Spiller, M.; Scrocca, A.; Bovera, F.; Rancilio, G. Modeling and Analysis of BESS Operations in Electricity Markets: Prediction and Strategies for Day-Ahead and Continuous Intra-Day Markets. *Sustainability* **2024**, *16*, 7940. [CrossRef]
8. Quan, R.; Liang, W.; Wang, J.; Li, X.; Chang, Y. An enhanced fault diagnosis method for fuel cell system using a kernel extreme learning machine optimized with improved sparrow search algorithm. *Int. J. Hydrogen Energy* **2024**, *50 Pt A*, 1184–1196. [CrossRef]
9. Reatti, A.; Balzani, M. PWM switch model of a buck-boost converter operated under discontinuous conduction mode. In Proceedings of the 48th Midwest Symposium on Circuits and Systems, Covington, KY, USA, 7–10 August 2005; Volume 1, pp. 667–670. [CrossRef]

10. Albertoni, L.; Grasso, F.; Matteucci, J.; Piccirilli, M.C.; Reatti, A.; Ayachit, A.; Kazimierczuk, M.K. Analysis and design of full-bridge Class-DE inverter at fixed duty cycle. In Proceedings of the IECON 2016—42nd Annual Conference of the IEEE Industrial Electronics Society, Florence, Italy, 24–27 October 2016; pp. 5609–5614. [CrossRef]
11. Quan, R.; Guo, H.; Liu, D.; Changab, Y.; Wana, H. Performance optimization of a thermoelectric generator for automotive application using an improved whale optimization algorithm. *Sustain. Energy Fuels* **2023**, *7*, 5528–5545. [CrossRef]
12. Bindi, M.; Grasso, F.; Luchetta, A.; Manetti, S.; Piccirilli, M.C. Smart Monitoring and Fault Diagnosis of Joints in High Voltage Electrical Transmission Lines. In Proceedings of the 2019 6th International Conference on Soft Computing & Machine Intelligence (ISCMI), Johannesburg, South Africa, 19–20 November 2019; pp. 40–44. [CrossRef]
13. Bindi, M.; Piccirilli, M.C.; Luchetta, A.; Grasso, F. A Comprehensive Review of Fault Diagnosis and Prognosis Techniques in High Voltage and Medium Voltage Electrical Power Lines. *Energies* **2023**, *16*, 7317. [CrossRef]
14. Velasquez, W.; Moreira-Moreira, G.Z.; Alvarez-Alvarado, M.S. Smart Grids Empowered by Software-Defined Network: A Comprehensive Review of Advancements and Challenges. *IEEE Access* **2024**, *12*, 63400–63416. [CrossRef]
15. Intravaia, M.; Becchi, L.; Bindi, M.; Paolucci, L.; Grasso, F. Autoencoders for Hourly Load Profile Reconstruction in Renewable Energy Communities. In Proceedings of the IEEE EUROCON 2023—20th International Conference on Smart Technologies, Torino, Italy, 6–8 July 2023; pp. 280–285. [CrossRef]
16. Belloni, E.; Bianchini, G.; Casini, M.; Faba, A.; Intravaia, M.; Laudani, A.; Lozito, G.M. An overview on building-integrated photovoltaics: Technological solutions, modeling, and control. *Energy Build.* **2024**, *324*, 114867. [CrossRef]
17. Sæle, H.; Morch, A.; Buonanno, A.; Caliano, M.; Somma, M.D.; Papadimitriou, C. Development of Energy Communities in Europe. In Proceedings of the 2022 18th International Conference on the European Energy Market (EEM), Ljubljana, Slovenia, 13–15 September 2022; pp. 1–5. [CrossRef]
18. Pasqui, M.; Becchi, L.; Bindi, M.; Intravaia, M.; Grasso, F.; Fioriti, G.; Carcasci, C. Community Battery for Collective Self-Consumption and Energy Arbitrage: Independence Growth vs. Investment Cost-Effectiveness. *Sustainability* **2024**, *16*, 3111. [CrossRef]
19. Salehi, N.; Martínez-García, H.; Velasco-Quesad, G.; Guerrero, J.M. A Comprehensive Review of Control Strategies and Optimization Methods for Individual and Community Microgrids. *IEEE Access* **2022**, *10*, 15935–15955. [CrossRef]
20. Stentati, M.; Paoletti, S.; Vicino, A. Optimization and Redistribution Strategies for Italian Renewable Energy Communities. In Proceedings of the IEEE EUROCON 2023—20th International Conference on Smart Technologies, Torino, Italy, 6–8 July 2023; pp. 263–268. [CrossRef]
21. Moncecchi, M.; Meneghello, S.; Merlo, M. Energy Sharing in Renewable Energy Communities: The Italian Case. In Proceedings of the 2020 55th International Universities Power Engineering Conference (UPEC), Turin, Italy, 1–4 September 2020; pp. 1–6. [CrossRef]
22. Cielo, A.; Margiaria, P.; Lazzeroni, P.; Mariuzzo, I.; Repetto, M. Renewable Energy Communities business models under the 2020 Italian regulation. *J. Clean. Prod.* **2021**, *316*, 128217. [CrossRef]
23. Zatti, M.; Moncecchi, M.; Gabba, M.; Chiesa, A.; Bovera, F.; Merlo, M. Energy Communities Design Optimization in the Italian Framework. *Appl. Sci.* **2021**, *11*, 5218. [CrossRef]
24. Hossain Lipu, M.S.; Ansari, S.; Miah, M.S.; Hasan, K.; Meraj, S.T.; Faisal, M.; Jamal, T.; Ali, S.H.M.; Hussain, A.; Muttaqi, K.M.; et al. A review of controllers and optimizations based scheduling operation for battery energy storage system towards decarbonization in microgrid: Challenges and future directions. *J. Clean. Prod.* **2022**, *360*, 132188. [CrossRef]
25. Henni, S.; Staudt, P.; Weinhardt, C. A sharing economy for residential communities with PV-coupled battery storage: Benefits, pricing and participant matching. *Appl. Energy* **2021**, *301*, 117351. [CrossRef]
26. Mustika, A.D.; Rigo-Mariani, R.; Debusschere, V.; Pachurka, A. A two-stage management strategy for the optimal operation and billing in an energy community with collective self-consumption. *Appl. Energy* **2022**, *310*, 118484. [CrossRef]
27. Secchi, M.; Barchi, G.; Macii, D.; Moser, D.; Petri, D. Multi-objective battery sizing optimisation for renewable energy communities with distribution level constraints: A prosumer-driven perspective. *Appl. Energy* **2021**, *297*, 117171. [CrossRef]
28. Pasqui, M.; Felice, A.; Messagie, M.; Coosemans, T.; Bastianello, T.T.; Baldi, D.; Lubello, P.; Carcasci, C. A new smart batteries management for Renewable Energy Communities. *Sustain. Energy Grids Netw.* **2023**, *34*, 101043. [CrossRef]
29. Namor, E.; Sossan, F.; Cherkaoui, R.; Paolone, M. Control of Battery Storage Systems for the Simultaneous Provision of Multiple Services. *IEEE Trans. Smart Grid* **2019**, *10*, 2799–2808. [CrossRef]
30. Qin, j.; Wan, Y.; Li, F.; Kang, Y.; Fu, W. *Distributed Economic Operation in Smart Grid: Model-Based and Model-Free Perspectives*; Springer Nature: Singapore, 2023.
31. Barchi, G.; Pierro, M.; Secchi, M.; Moser, D. Residential Renewable Energy Community: A Techno-Economic Analysis of the Italian Approach. In Proceedings of the 2023 IEEE International Conference on Environment and Electrical Engineering and 2023 IEEE Industrial and Commercial Power Systems Europe (EEEIC/I&CPS Europe), Madrid, Spain, 6–9 June 2023; pp. 1–6. [CrossRef]
32. Becchi, L.; Bindi, M.; Intravaia, M.; Grasso, F.; Pasqui, M.; Carcasci, C. Application of Control Algorithms for Battery Scheduling in Grid-Connected Energy Prosumers. In Proceedings of the 2024 IEEE 22nd Mediterranean Electrotechnical Conference (MELECON), Porto, Portugal, 25–27 June 2024; pp. 932–937. [CrossRef]

33. Patalas-Maliszewska, J.; Szmołda, M.; Łosyk, H. Integrating Artificial Intelligence into the Supply Chain in Order to Enhance Sustainable Production—A Systematic Literature Review. *Sustainability* **2024**, *16*, 7110. [CrossRef]
34. Li, X.; Wang, Q.; Tang, Y. The Impact of Artificial Intelligence Development on Urban Energy Efficiency—Based on the Perspective of Smart City Policy. *Sustainability* **2024**, *16*, 3200. [CrossRef]
35. Salama, R.; Al-Turjman, F. Sustainable Energy Production in Smart Cities. *Sustainability* **2023**, *15*, 16052. [CrossRef]
36. Doran, N.M.; Badareu, G.; Doran, M.D.; Enescu, M.; Staicu, A.L.; Niculescu, M. Greening Automation: Policy Recommendations for Sustainable Development in AI-Driven Industries. *Sustainability* **2024**, *16*, 4930. [CrossRef]
37. Zhang, Y. *Solving Large-Scale Linear Programs by Interior-Point Methods Under the MATLAB Environment*; Technical Report TR96-01; Department of Mathematics and Statistics, University of Maryland: Baltimore, MD, USA, 1995.
38. Deng, L.; Zhang, X.; Yang, T.; Sun, H.; Fu, Y.; Guo, Q.; Oren, S.S. Energy Management of Price-Maker Community Energy Storage by Stochastic Dynamic Programming. *CSEE J. Power Energy Syst.* **2024**, *10*, 492–503. [CrossRef]
39. Guan, Y.; Wei, B.; Guerrero, J.M.; Vasquez, J.C.; Gui, Y. An overview of the operation architectures and energy management system for multiple microgrid clusters. *iEnergy* **2022**, *1*, 306–314. [CrossRef]
40. Wang, Z.; Chen, A.; Wang, N.; Liu, T. Multi-Objective Operation Optimization Strategy for Integrated Community Energy Systems Considering Demand Side Management. *IEEE Trans. Ind. Appl.* **2024**, *60*, 1332–1344. [CrossRef]
41. Mustika, A.D.; Rigo-Mariani, R.; Debusschere, V.; Pachurka, A. Self-Consumption and Frequency Reserve Provision with Energy Communities. *IEEE Access* **2023**, *11*, 83666–83679. [CrossRef]
42. Scarabaggio, P.; Carli, R.; Jantzen, J.; Dotoli, M. Stochastic Model Predictive Control of Community Energy Storage under High Renewable Penetration. In Proceedings of the 2021 29th Mediterranean Conference on Control and Automation (MED), Puglia, Italy, 22–25 June 2021; pp. 973–978. [CrossRef]
43. Srithapon, C.; Månsson, D. Predictive control and coordination for energy community flexibility with electric vehicles, heat pumps and thermal energy storage. *Appl. Energy* **2023**, *347*, 121500. [CrossRef]
44. Shamim, N.; Subburaj, A.; Bayne, S. Model Predictive Control Analysis for the Battery Energy Storage System. In Proceedings of the 2017 Ninth Annual IEEE Green Technologies Conference (GreenTech), Denver, CO, USA, 29–31 March 2017; pp. 34–38. [CrossRef]
45. Khalid, M.; Savkin, A.V. Model predictive control based efficient operation of battery energy storage system for primary frequency control. In Proceedings of the 2010 11th International Conference on Control Automation Robotics & Vision, Singapore, 7–10 December 2010; pp. 2248–2252. [CrossRef]
46. Hu, J.; Shan, Y.; Guerrero, J.M.; Ioinovici, A.; Chan, K.W.; Rodriguez, J. Model predictive control of microgrids—An overview. *Renew. Sustain. Energy Rev.* **2021**, *136*, 110422. [CrossRef]
47. Baños, R.; Manzano-Agugliaro, F.; Montoya, F.G.; Gil, C.; Alcayde, A.; Gómez, J. Optimization methods applied to renewable and sustainable energy: A review. *Renew. Sustain. Energy Rev.* **2011**, *15*, 1753–1766. [CrossRef]
48. Lazzari, F.; Mor, G.; Cipriano, J.; Solsona, F.; Chemisana, D.; Guericke, D. Optimizing planning and operation of renewable energy communities with genetic algorithms. *Appl. Energy* **2023**, *338*, 120906. [CrossRef]
49. Wang, H.; Meng, K.; Dong, Z.Y.; Xu, Z.; Luo, F.; Wong, K.P. Efficient real-time residential energy management through MILP based rolling horizon optimization. In Proceedings of the 2015 IEEE Power & Energy Society General Meeting, Denver, CO, USA, 26–30 July 2015; pp. 1–6. [CrossRef]
50. Wu, D.; Gui, Q.; Zhao, W.; Wang, J.; Shi, S.; Zhou, Y. Battery Energy Storage System (BESS) Sizing Analysis of Bess-Assisted Fast-Charge Station Based on Double-Layer optimization Method. In Proceedings of the 2020 IEEE 3rd Student Conference on Electrical Machines and Systems (SCEMS), Jinan, China, 4–6 December 2020; pp. 658–662. [CrossRef]
51. Jia, L.; Pannala, S.; Srivastava, A. Enhancing Resilience in Islanded Microgrids with PV-Battery using Bi-level MILP Optimization. In Proceedings of the 2023 IEEE International Conference on Energy Technologies for Future Grids (ETFG), Wollongong, Australia, 3–6 December 2023; pp. 1–6. [CrossRef]
52. Wang, H.; Abdollahi, E.; Lahdelma, R.; Jiao, W.; Zhou, Z. Modelling and optimization of the smart hybrid renewable energy for communities (SHREC). *Renew. Energy* **2015**, *84*, 114–123. [CrossRef]
53. Talluri, G.; Lozito, G.M.; Grasso, F.; Iturrino Garcia, C.; Luchetta, A. Optimal Battery Energy Storage System Scheduling within Renewable Energy Communities. *Energies* **2021**, *14*, 8480. [CrossRef]
54. Nagpal, H.; Avramidis, I.; Capitanescu, F.; Madureira, A.G. Local Energy Communities in Service of Sustainability and Grid Flexibility Provision: Hierarchical Management of Shared Energy Storage. *IEEE Trans. Sustain. Energy* **2022**, *13*, 1523–1535. [CrossRef]
55. Liu, Y.; Hu, S. Renewable Energy Pricing Driven Scheduling in Distributed Smart Community Systems. *IEEE Trans. Parallel Distrib. Syst.* **2017**, *28*, 1445–1456. [CrossRef]
56. Available online: https://www.ausgrid.com.au/ (accessed on 1 October 2024).
57. Available online: https://planetsmartcity.it/ (accessed on 1 October 2024).
58. Available online: https://joint-research-centre.ec.europa.eu/photovoltaic-geographical-information-system-pvgis_en (accessed on 1 October 2024).

59. Available online: https://www.gse.it/ (accessed on 1 October 2024).
60. Becchi, L.; Bindi, M.; Intravaia, M.; Sabino, L.; Garzon Alfonso, C.C.; Grasso, F.; Riganti Fulginei, F.; Crescimbini, F. Low-Complexity Neural Networks for Electrical Load Forecasting in Renewable Energy Communities. In Proceedings of the 2024 IEEE International Symposium on Consumer Technology (ISCT), Bali, Indonesia, 13–16 August 2024.